An Ingenious Pressure Surveillance Algorithm to Detect CO_2 Ingress Accidents in a Sodium-cooled Fast Reactor

Dong-Won LIM[1], Jaehyuk EOH[1]*, and Ji-Young JEONG[1]

1. SFR System Design Div., Korea Atomic Energy Research Institute, Daedeok-daero 989-111, Yuseong-gu, Daejeon, 34057, Korea

**** Corresponding author (Tel: +82-42-868-8970, E-mail: jheoh@kaeri.re.kr)***

Abstract: The supercritical CO_2 Brayton cycle employed in Sodium-cooled Fast Reactors (SFRs) is more advantageous than a conventional Rankine cycle energy conversion system. One of the benefits is an enhanced plant safety since potential reactions of CO_2 with liquid sodium have been reported to be less stringent than a sodium-water reaction (SWR) anticipated in the Rankine cycle, and CO_2 reactions also take more chemical reaction time than an SWR. Contradictorily, the reaction characteristics of CO_2 require a scrupulous plant operation. Moderate chemical interactions between CO_2 and liquid sodium imply that detecting CO_2 ingress accidents (unlike conspicuous physical indications such as noisy wastage due to SWR) makes it hard to detect at its early stage. In other words, the plant can run for an extended period of time until the rupture disk bursts, letting a damaged sodium-to-CO_2 heat exchanger degrade further. To detect CO_2 ingress accidents, this paper proposes an ingenious approach to compare the pressure measurements in real time of two identical heat exchangers, which are in a typical SFR configuration. The approach was originated from the ideas that the CO_2 ingress—a source of pressure transient in a loop—occurs owing to a crack at the pressure boundary wall of a sodium-to-CO_2 heat exchanger, a certain self-recovery of structural damage does not happen over time, and probabilistically, an accident occurs at only one component out of two at the first place. This pressure surveillance algorithm by which the threshold and decision time parameters can be determined is based on probabilistic performance analysis by setting false alarm and true detection rates. The decision time is chosen to be sufficiently long to allow a particular ingress level can be detected even in the presence of asymmetric performances of the two heat exchangers. Finally, the proposed algorithm was developed with a simplified mass and energy transfer (SMET) model, and verified with experimental data obtained from a water mock-up test. The results show that 99.99% detection probability can be achieved for 30 cc/sec air ingress, which is equivalent to 0.12 g/sec CO_2 ingress, using a detection time of less than 70 seconds, limiting down to 0.1% false alarms due to sensor noise.

Keyword: Sodium-CO_2 chemical reaction, CO_2 Brayton cycle, Pressure monitoring, Double redundancy monitoring, Probabilistic performance analysis

1 Introduction

A potential sodium fire or sodium-water reaction (SWR) is envisaged as a critical event for the safety of sodium-cooled fast reactors (SFRs). SWR occurs in a steam generator (SG) unit where hot sodium coolant of the intermediate heat transport loop (IHTS) in an SFR exchanges heat with water to generate steam for turbine input (refer to Fig. 1). Sodium reacts rapidly with steam/water, generating heat and rapid pressure pulse which can lead to the catastrophic failure of an SG unit and intermediate sodium loop by over-pressure and temperature transients.

Some of major SWR accidents reported in literature are briefly reviewed. The first SWR in PHENIX was 30 kg of water reacted [1]. The worst tube leak event in SGs of PFR (Prototype Fast Reactor) occurred in 1987 [2]. Thirty-nine tubes around the initial tube within 10 seconds were broken through during the time required for the pressure decrease on the steam side (rupture disk was broken). Significant SWR events occurred in BN-350 (detected by a satellite) and BN-600

(the most important reaction took place in January 1981 with 40 kg of water injected) [3].

To detect SWR events at its early stage, hydrogen detection is used, because hydrogen as SWR byproducts is created and transported in a sodium loop [4-5]. However, indispensable reliability and quickness of the hydrogen detection system is challenging, for hydrogen byproducts tend to travel along with the coolant in the loop, and it is not relatively easy to capture it to measure. Design of a wrapper around the free-standing SG, which is capable to withstand the most violent SWR, was proposed. This will eventually increase design and manufacturing costs, and large SWR accidents are in any case undesirable regardless of wrapper features. Rupture disk (R/D) membranes are designed to limit pressure accumulation to avoid high internal pipe pressure in the loop and its consequential ruptures. When rupture disk is broken, however, the secondary sodium coolant will be immediately drained from the loop. At the rupture break burst, the last measure to protect the reactor from SWR, the damage may have gotten developed aggressively, and this leads to the long-term shutdown. This is a huge economic loss in operation and plant management.

Employing CO_2 gas as an alternative matter replacing steam/water in an SG, the SG with the supercritical CO_2 Brayton cycle shown in Fig. 1 is advantageous in a couple of ways compared with the conventional Rankine cycle SG [6]. In addition to its high thermal efficiency and its potential compactness of the heat-exchanger system with the CO_2 Brayton cycle [6-7], it can be a safer system than an SFR with conventional SGs. A sodium-CO_2 reaction is claimed to be milder than an SWR [7-9]. Referring to [10], the liquid sodium and CO_2 gas is categorized as a rate-controlled process, because its reaction rate strongly depends on the reaction condition, and the chemical reaction speed between sodium and CO_2 gas is consequently much slower than that of an SWR.

However, it is contradiction that a scrupulous operation of the plant is required due to the reaction characteristics of CO_2. Moderate chemical interactions between CO_2 and sodium imply that detecting CO_2 ingress accidents, which may not be like conspicuous physical indications in SWRs such as noisy wastage, makes it hard to detect at its early stage. In other words, the SGs, damaged sodium-CO_2 heat exchangers, can run for an extended period of time, and degrade further until the rupture disk breaks.

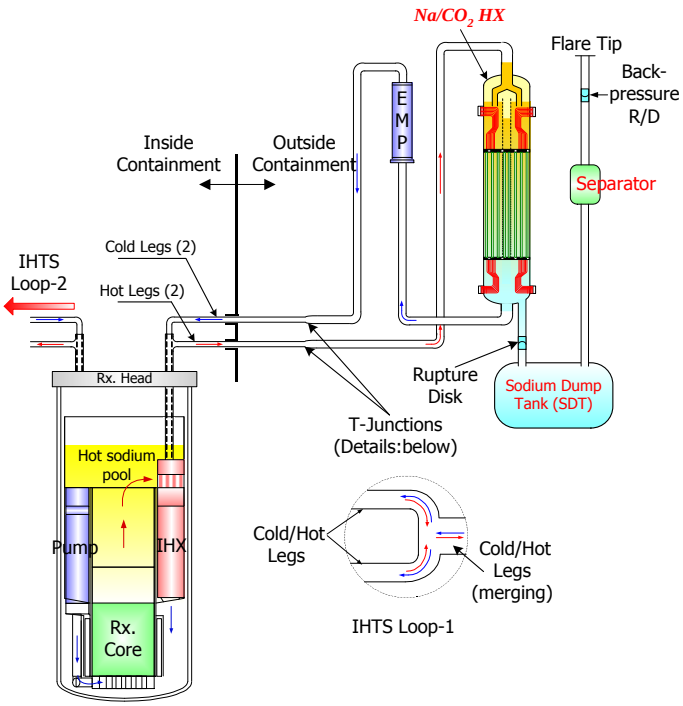

Fig. 1 Schematic diagram of KALIMER-600 [13] heat transport system

Roine [11] studied sodium and carbon dioxide chemical interactions. Among a couple of reactions, C-CO_2 and Na-CO_2 interactions produce gaseous byproduct, carbon monoxide (CO). CO byproducts and unreacted portion of CO_2 ingress gases increase the pipe internal pressure. Eventually, as the pressure reaches a certain design level (approximately 1~2 MPa, which is greater than 10 times the cover-gas pressure), the rupture disk is broken to evacuate the sodium coolant in a loop to the sodium dump tank (SDT).

Before R/D is torn apart by the CO_2 ingress accident, automatic shutdown accompanied with a quick depressurization in the CO_2 gas side is

desirable. Stopping CO_2 gas supply to SGs is a better strategy to mitigate SG damage than relying solely on R/Ds. Draining sodium may not be necessary, when the failure is detected early, and CO_2 can be quickly injected once the damage is repaired. But, it is a question whether the CO_2 ingress can be detected by pressure measurements alone before R/D is broken. Moreover, the way to calculate the threshold level and time to trigger the CO_2 removal at an early damage stage is required.

The goal of this study is to bring about a mathematical framework based on physics to automatically depressurize the steam side, and disconnect water supply by detecting localized sodium-CO_2 events in SGs. Previously, it was studied that generated hydrogen amount increases internal loop pressure in a fairly short period of time, and this pressure surge is less dependent on the loop flow rate or disturbed flow by an in-flow obstacle [12]. Thus, a less intrusive surveillance approach using only global metrics in pressure is taken to monitor more than 1400 tubes for two SGs. The proposed framework makes it available to estimate the detection time of CO_2 ingress due to the target damage size of micro or small leak rates (self-wastage level of approximately 10^{-1}~1 g/s).

For the pilot study, experimental results from the simplified mass and energy transfer (SMET) model were adopted to evaluate the proposed mathematical framework, which allows the calculation of the achievable minimum time for given in-let flow rates.

2 Problem Formulation

Since the intermediate heat transport system connecting the reactor to SGs is a closed loop, the pressure and temperature transients in the cover gas area of an expansion tank of the loop represent the dynamic behavior of the loop as a whole [12]. Therefore, once a relationship between the cover-gas pressure and mass flow rate into the loop due to the CO_2 ingress is determined, the SG failure can be monitored by cover-gas pressure measurements. The description of the relation can be proceeded from the energy balance between the cover gas and the shell-side sodium as a simplified mass and energy transfer (SMET) model (Fig. 2) developed in [9].

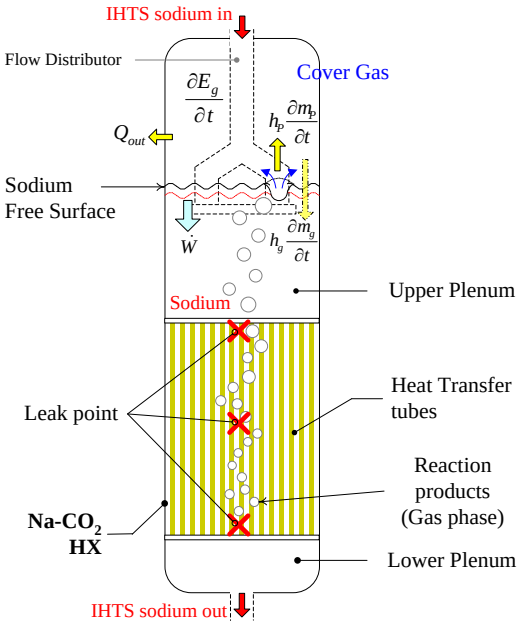

Fig. 2 Energy balance of the cover gas region (SMET model) [9]

For the SMET model, authors of [9] developed a mathematical representation and have shown its validity [9]. Referring to the thermo-dynamic relation for the pressure P_g in the cover gas region from the same paper, it is expressed as

$$\frac{dP_g}{dt} = \frac{\bar{R}}{M_p} \cdot \frac{T_g}{V_g}\left(\frac{\partial m_p}{\partial t}\right) + \left(\frac{m_p^{acc}}{M_p^0} + \frac{m_g^0}{M_g^0}\right) \cdot \frac{\bar{R}}{V_g} \cdot \frac{dT_g}{dt} - \frac{P_g}{V_g} \cdot \frac{dV_g}{dt} \quad (1)$$

Note the full derivation of the above Eq. (1) is described in [9]. In Eq. (1), the subscript p and g stand for byproducts due to the reactions and cover gas, respectively. M, $\bar{R}$, T, V, m, and t represent the molecular weight, universal gas constant (8.314 [kJ/kmol-K]), temperature [K], volume [m^3], mass [kg], and time [sec], respectively. $m_p^{acc}$is the accumulated byproducts in the cover gas, and the superscript 0 means an initial or reference state. During the process, the cover gas volume changes little relatively in the early stage of reactions, and thus the time

derivative term of V_g is taken to be zero. Molecular weights do not change over time, and the cover-gas mass is assumed to be conserved ($m_g^0 = m_g$ all the time).

Thus, Eq. (1) can be approximated in discrete time j with a very small sampling time Δt in a forward difference-equation form as

$$\frac{P_g^{j+1}-P_g^j}{\Delta t} = \zeta\left(\frac{m_p^{j+1}-m_p^j}{\Delta t}\right)T_g^{j+1} + \left(m_p^{acc}\zeta + m_g\xi\right)\left(\frac{T_g^{j+1}-T_g^j}{\Delta t}\right), \quad (2)$$

where

$$\zeta = \frac{\bar{R}}{V_g M_p} \quad \left[\frac{J}{m^3 gK}\right], \quad (3)$$

$$\xi = \frac{\bar{R}}{V_g M_g} \quad \left[\frac{J}{m^3 gK}\right]. \quad (4)$$

In early times of reaction, m_p^{acc} can be relatively negligible to the cover-gas mass m_g. Eq. (2) can be re-organized, having m_p^{acc} neglected, as of following

$$P_g^{j+1} = P_g^j + m_g\xi\left(T_g^{j+1} - T_g^j\right) + \zeta\left(m_p^{j+1} - m_p^j\right)T_g^{j+1}. \quad (5)$$

Define the damage term g_D as a multiplicative constant for a limited period of time as

$$g_D = \zeta\left(m_p^{j+1} - m_p^j\right) = \zeta\dot{m}_p\Delta t \quad (6)$$

where $\dot{m}_p$ is the byproduct generation rate in g/sec due to CO_2 ingress. Thus, Eq. (5) can be further simplified into

$$P^{j+1} = P^j + m\xi\left(T^{j+1} - T^j\right) + g_D T^{j+1}. \quad (7)$$

In the equation, the subscript g was dropped for convenience, because only the cover gas region is of interest.

3 Pressure Surveillance Algorithm

The method for the pressure surveillance algorithm is derived by probabilistic analysis. From Eq. (7), the cover gas pressure as a time propagation model can be constructed as

$$P^{j+1} = P^j + B^{j+1} + g_D T^{j+1} \quad (8)$$

where

$$B^{j+1} = m_g\xi\left(T_g^{j+1} - T_g^j\right) \quad (9)$$

and B^j is the cover gas pressure compensation term due to temperature variation at time step j.

A scheme to monitor CO_2 ingress accidents is to compare the pressure measurements of two identical systems at the same time. This strategy assumes that two identical steam generators are used in a reactor plant, which is a general deployment. It is also grounded upon other assumptions that two heat transport systems are under a similar working condition, and it is very unlikely that two systems fail at the same time with the same damage degree. Assumptions are reasonable, because two systems are designed to be identical, are connected to one reactor, and work at the same site, but a typical breakage failure between a shell- and tube-side may be caused by manufacturing faults which are random.

A residual r is defined for the comparison between heat transport system 1 and 2. For r, pressure measurements from two target devices are subtracted from each other.

$$r^j = P_1^j - P_2^j \quad (10)$$

The difference between sensor measurements, considering its noise factor and variations due to slight different working environment, can be modeled as a random variable δ in a normal distribution function. Also, for this initial study, the difference between temperature propagation terms B_1 and B_2 is regarded as a system variation which is included in δ. The measurement variation δ is between two healthy systems, and the damage term has to be accumulated in time. Suppose only the system 1 is faulted from time *js* until *jf*. Then, the Eq. (10) can be expressed from Eq. (7) as

$$r^j = P_1^j - P_2^j = \delta + \sum_{js}^{jf} g_D T_1^j \qquad (11)$$

where

$$\delta \sim N(0, \sigma^2) \qquad (12)$$

The inspection is carried out after every decision time k_d interval as follows:

Statement 1.

- If $-\mathrm{L} < r < L$ at k_d,
  → no failure is declared.
- If $r \leq -L$ or $r \geq L$ at k_d,
  → a detection of a failure due to ingress accidents is declared.

Inspections are performed at every k_d time (seconds). In other words, to detect the failure, it has to be waited for k_d seconds, and even if high (or low) r value is found in between, it is not declared as being "detected", for it is highly likely to be a noise. This scheme is strongly dependent on the hydro-dynamic behavior of the cover-gas region expressed in Eq. (1) and its damage model in Eq. (11).

A constant mass flow rate from reaction was assumed, and an average temperature $\overline{T_1}$ is taken. When a reaction starts from time j = 1 to k, Eq. (11) becomes

$$r^k = P_1^k - P_2^k = \delta + k g_D \overline{T_1} \qquad (13)$$

When there is no damage in a system ($g_D = 0$), the residual r for monitoring is centered around its average 0 as a bell-curve shape shown in Fig. 3. The figure shows two curves with small and large variances ($\sigma_1^2 < \sigma_2^2$). The probability of false alarming is the integral of the probability density curve in the outside of the threshold level $[-L, L]$. L is solved for by having an allowable false alarm rate, which should be very small. For the same false alarm rate, the threshold range for greater variance should be wider as in the figure ($L_1 < L_2$).

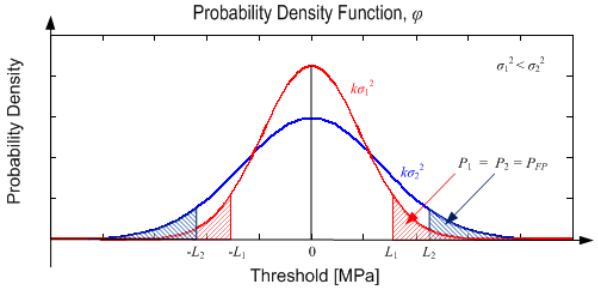

Fig. 3 Probability density function of a normal distribution model for a comparison between two variance values

But, when there is a fault in a system ($g_D \neq 0$), the bell-curve is shifted as much as the mean-value contribution $k g_D \overline{T_1}$ as shown in Fig. 4. The figure shows two different detection time ($k_1 < k_2$). The probability of true detection for this scenario is the area under the density function curve in the outside the threshold level $[-L, L]$. Therefore, with longer waiting to detect the same amount of a fault, the probability of detection increases as illustrated in the figure (the area for k_2 is greater than for k_1).

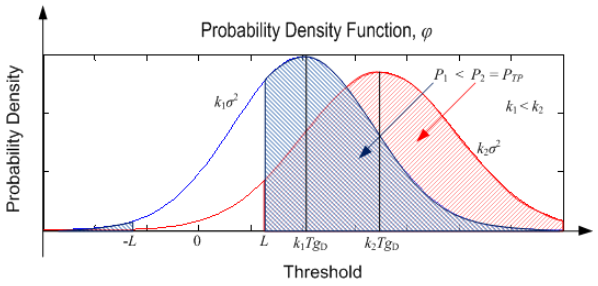

Fig. 4 Probability density function of a normal distribution model for a comparison between two mean values

To design the monitoring system (mainly for the threshold level L and detection time k_d), parameters of the statistics information of sensors and target damage size should be determined with probability inputs $p_{FP,max}$ and $p_{TP,min}$ (max. allowed false alarm and least required true detection probabilities). The least L and soonest k_d are calculated based on the probability model in Eqs. (11-13) and descriptions given earlier as follows in Eqs. (14) and (15).

$$P\left(\left|r_{k_d}\right| \geq L \mid g_D = 0\right) = 1 - \int_{-L}^{L} \frac{1}{\sqrt{2\pi\sigma^2}} exp^{-\frac{x^2}{2\sigma^2}} dx \leq p_{FP,max} \quad (14)$$

$$P\left(\left|r_{k_d}\right| \geq L \mid g_D \neq 0\right) = 1 - \int_{-L}^{L} \frac{1}{\sqrt{2\pi\sigma^2}} exp^{-\frac{\left(x-g_D k_d \bar{T}\right)^2}{2\sigma^2}} dx \geq p_{TP,min} \quad (15)$$

Again, $p_{FP,,max}$ is a very small number such as one in 1000 inspections, and $p_{TP,,min}$ is close to 1 such as 99.99%.

4 Experiments and Simulation

The monitoring strategy was verified for the first time with the water mock-up test facility introduced in [9] (Fig. 5). With using this facility and data, the sodium/carbon dioxide reaction by CO_2 ingress accidents was simulated with an air injected into the water loop that corresponds to the sodium heat transport system. For the verification, the monitoring system is to detect the air injection. The design of the system is explained with the results for the air detection.

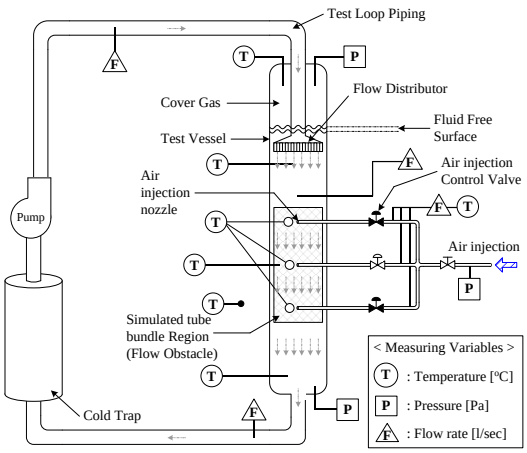

Fig. 5 Schematic drawing of the test facility in [12]

For the data acquisition setting, the sampling time Δt is set as 0.2 second. Because the byproduct (injected air, here) and cover gas are air and the cover gas volume is 5.38 liters, the environmental constants, ζ and ξ, in [J/m^3-g-K] are

$$\zeta = \xi = \frac{\bar{R}}{V_g M_{air}} = \frac{8.314}{5.38 \cdot 28.8} \cdot 10^3 = 53.6581. \quad (16)$$

The average temperature $\bar{T}$ of the cover gas region is 286 K.

In order to take advantage of the test facility, the monitoring scheme is constructed to compare the cover-gas pressure with its statistical mean μ, and from Eq. (13) the residual becomes,

$$r^k = P_{test}^k - \mu = \delta + k g_D \bar{T} \quad (17)$$

and

$$\delta \sim N(0, \sigma^2) \quad (18)$$

The inspection is carried out after every decision time k_d interval as described in the *statement* 1.

4.1 Threshold *L* Determination

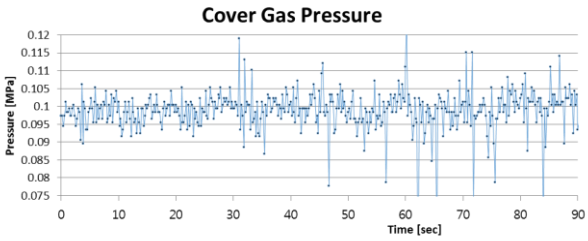

Fig. 6 Pressure measurements when no air is injected

In Fig. 6, pressure measurements for a dry run of 90 seconds without air injection are given. The data is used for extracting the statistics information of the loop (system) including sensor dynamics: statistical mean μ and standard deviation σ.

$$\mu = 9.9054 \cdot 10^{-2} \text{ [MPa]} \quad (19)$$

$$\sigma = 6.5184 \cdot 10^{-3} \text{ [MPa]} \quad (20)$$

To minimize false alarm when no fault, the threshold level was set by the above statistics information and allowable false positive rate of 0.1%.

$$1 - \int_{-L}^{L} \frac{1}{\sqrt{2\pi\sigma^2}} exp^{-\frac{x^2}{2\sigma^2}} dx \leq 0.001 \quad (21)$$

and the calculated threshold level L is obtained as

$$L = 0.014 \text{ [MPa]}. \quad (22)$$

4.2 Decision-time k_d Determination

The decision time k_d is calculated by the target damage level g_D converted from the air injection flow rate. The air is injected in a rate of 30 cc/s. Thus, the air mass flow rate, converted from its density at a 286 K temperature, and the damage factor become

$$\dot{m}_{air} = 30 \times 10^{-6} \times 1.225 \times 10^{3} = 0.03675 \text{ [g/sec]} \quad (23)$$

$$g_D = \zeta \dot{m}_{air} \Delta t = 0.3944, \quad (24)$$

With the mass flow rate of the air, an equivalent fault level of CO_2 ingress can be estimated. It is reported that the generation rate of CO gas is far less than 30% of the total of the released CO_2 gas [9]. But, conservatively, $\dot{m}_{air}$ is divided by 0.3, as $\dot{m}_{air}$ is a substitute of CO gas. Then, an equivalent mass flow rate of CO_2 gas for 0.03675 g/sec in Eq. (23) becomes ~0.12 g/sec.

Substituting values of the obtained parameters: L in Eq. (22), σ in Eq. (20), g_D in Eq. (24), $\bar{T} = 286$ K, and the minimum required detection probability of 99.99%; the detection time k_d is solved for from Eq. (25).

$$\int_{-L}^{L} \frac{1}{\sqrt{2\pi\sigma^2}} exp^{-\frac{(x-g_D k_d \bar{T})^2}{2\sigma^2}} dx \geq 0.9999, \quad (25)$$

and

$$k_d = 67.8 \text{ [sec]}. \quad (26)$$

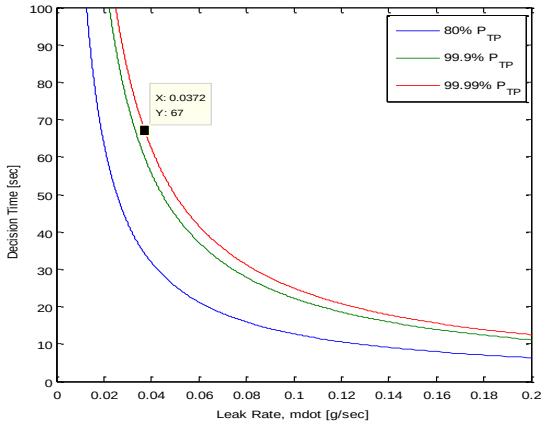

Fig. 7 Calculated decision times for various leak rates (damage levels)

A range of various leak rate including the air mass flow value in Eq. (23) is simulated from the relation in Eq. (25). The plot in Fig. 7 gives the results of the decision time for the leak-rate range. As expected, a longer detection time is required for a small leak rate (damage) than a large one. In other words, for a large damage, the detection time required is very short. Furthermore, for a comparison, the figure contains three cases of $p_{TP,min}$: 80%, 99.9%, and 99.99%. For a same amount of damage, a longer detection is required for a higher probability as depicted in the figure. A sample value, for example, of a leak rate 0.0372 g/sec is marked, having 67 seconds of the detection time in the figure.

Its decreasing pattern of Fig. 7 is exponential, meaning very small damage less than 0.01 g/sec is almost impossible to detect, considering the plant operation and other extraneous effects. It takes also too long (such as 5 minutes) to run a system effectively. This long interval is not able to find an incipient failure, and thus the very small damage is not an appropriate target.

4.3 Case Study

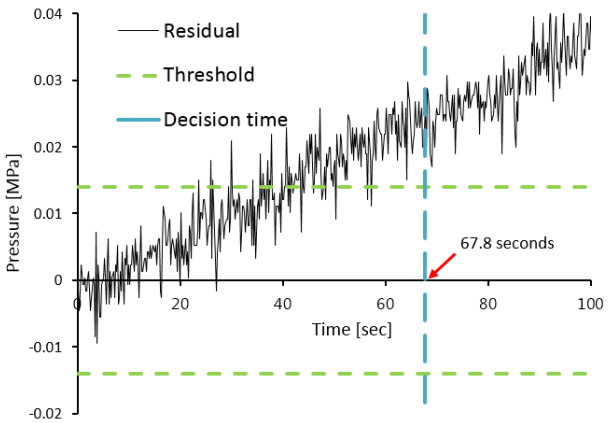

Fig. 8 A sample case study for the pressure surveillance algorithm verification: The air injection was detected at the calculated threshold level and detection time.

A sample case study is taken out of air-injection tests performed in [12]. The residual by pressure measurement data as a black curve of Fig. 8 was compared with the calculated L (green dashed line) at k_d (blue dashed line) time. The mean $\mu = 9.9054 \cdot 10^{-2}$ MPa was subtracted from the

pressure to yield a residual as in Eq. (17). As shown in Fig. 8, at the calculate k_d of 67.8 seconds, 30 cc/sec of air injection into the water mock-up test facility was able to be detected with 99.99% detection probability. The measured pressure is 0.1249 MPa at 67.8 sec, and the residual ($0.1249 - 0.09905 = 0.02585$ MPa) is greater than the upper threshold L of 0.014 MPa.

5 Conclusions

A pressure surveillance algorithm by probabilistic analysis to detect a structural failure due to CO_2 ingress accidents was developed. The scheme, comparing the cover gas pressure measurements of a redundant system, could detect anomalies of sodium-CO_2 heat exchangers.

The threshold and decision time parameters for this pressure surveillance algorithm were probabilistically calculated from statistics information of measurements by setting false alarm and true detection rates. The threshold allows statistic variations of measurements to reduce false alarming, when there is no fault. The decision time is chosen to be sufficiently long to detect a particular damage level with a high probability of detection, when there is a fault in one system.

To verify the algorithm, water mock-up experimental results were taken. In verification by using the water test facility, the byproducts due to CO_2 ingress were simulated by the air injection. The scheme was modified into comparing pressure values with the average of measurements at times when the air is not injected.

To allow signal noise, the threshold level of 0.014 MPa was calculated to minimize down to 0.1% false alarm rate (one false alarm out of 1000 inspection times). With 0.065 MPa sensor noise (standard deviation), the 30 cc/sec air injection, which is equivalent to the CO_2 ingress rate of 0.12 g/sec, was able to be detected at a decision time of 67.8 seconds with 99.99% detection probability.

Acknowledgement

This study was supported by the Ministry of Science, ICT, and Future Planning of South Korea through National Research Foundation funds (National Nuclear Technology Program, No. 2012M2A8A2025635).

References

[1] J.-F. Parisot, France, and Commissariat à l'énergie atomique et aux énergies alternatives, Sodium-cooled nuclear reactors. 2016.

[2] J. Guidez and L. Martin, "Lessons learned from sodium-cooled fast reactor operation and their ramifications for future reactors with respect to enhanced safety and reliability," Nuclear Technology, Vol. 164, pp. 207-220, Nov. 2008.

[3] "Unusual occurrences during LMFR operation," Proc. Technical Committee Meeting, Vienna, Austria, Nov. 9-13, 1998, IAEA-TECDOC-1180, International Atomic Energy Agency, 2000.

[4] M. Saez, S. Menou, A. Allou, F. Beauchamp, C. Bertrand, G. Rodriguez, and G. Prele, "Sodium-Water Reaction approach and mastering for ASTRID Steam Generator design," In Proceedings of IAEA FR13 Meeting, 2013.

[5] V. Nema, D. Sujish, B. Muralidharan, M. Rajan, and G. Vaidyanathan, Dynamics of hydrogen in sodium in LMFBR secondary circuit, 2006.

[6] V. Dostal, M. J. Driscoll, and P. Hejzlar, "A supercritical carbon dioxide cycle for next generation nuclear reactors," MIT-ANP-TR-100, 2004.

[7] J. J. Sienicki et. al, "Utilization of the supercritical CO_2 Brayton cycle with Sodium-cooled fast reactors," The 4th International Symposium - Supercritical CO2 Power Cycles, Pittsburgh, Pennsylvania, Sep., 2014,

[8] C. Latge, G. Rodriguez, and N. Simon, "Supercritical CO2 Brayton cycle for SFR Na-CO2 interaction and consequences on design and operation," GLOBAL 2005: Proceedings of the international conference on nuclear energy systems for future generation and global sustainability, pp. 2562, Japan, 2005.

[9] J.-H. Eoh,, J.-Y. Jeong, J.-W. Han, S.-O. Kim, "Numerical simulation of a potential CO2 ingress accident in a SFR employing an advanced energy conversion system," Annals of Nuclear Energy, Dec 31, 35(12), pp. 2172-2185, 2008.

[10] J.M. Smith, H.C. Van Ness, Introduction to Chemical Engineering Thermodynamics, third ed. McGraw-Hill Book Company, New York, 1975.

[11] A. Roine, Chemical reaction & equilibrium software with extensive thermo-chemical database, Outokumpu HSC Chemistry for Windows, Version 5.1, 2002.

[12] J.H. Eoh, J.Y. Jeong, S.O. Kim, D. Hahn, N.C. Park, "Development and experimental verification of the numerical simulation method for the quasi-steady SWR phenomena in a LMR steam generator," Nuclear Technology, Vol. 152, pp. 286–301, 2005.

[13] Y.-i. Kim, et al., "Design Concept of Advanced Sodium-Cooled Fast Reactor and Related R&D in Korea," Science and Technology of Nuclear Installations, Vol. 2013, 2013.